

See discussions, stats, and author profiles for this publication at: <https://www.researchgate.net/publication/263897951>

# Blue, Green, and Orange–Red Emission from Polystyrene Microbeads for Solid–State White–Light and Multicolor Emission

Article in *The Journal of Physical Chemistry B* · July 2014

DOI: 10.1021/jp504718m · Source: PubMed

CITATIONS

8

READS

169

2 authors:



Swapnil L Sonawane

CSIR - National Chemical Laboratory, Pune

4 PUBLICATIONS 19 CITATIONS

[SEE PROFILE](#)



Asha S. K

CSIR - National Chemical Laboratory, Pune

58 PUBLICATIONS 677 CITATIONS

[SEE PROFILE](#)

Some of the authors of this publication are also working on these related projects:



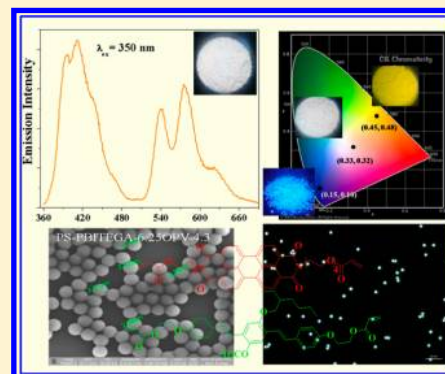
fluorescent molecularly imprinted polymers [View project](#)

# Blue, Green, and Orange-Red Emission from Polystyrene Microbeads for Solid-State White-Light and Multicolor Emission

Swapnil L. Sonawane<sup>†,‡</sup> and S. K. Asha<sup>\*,†,‡,§</sup><sup>†</sup>Polymer Science and Engineering Division, CSIR-National Chemical Laboratory, Dr. Homi Bhabha Road, Pune 411008, India<sup>‡</sup>Academy of Scientific and Innovative Research, Delhi – Mathura Road, New Delhi 110025, India<sup>§</sup>CSIR-Network Institutes of Solar Energy, New Delhi 110012, India

## Supporting Information

**ABSTRACT:** Solid-state white-light emission was achieved from polystyrene (PS) microbeads incorporated with fluorophores based on perylene bisimide (PBITEG) and oligo(*p*-phenylenevinylene) (OPV) as acrylic cross-linkers. The PS beads incorporated with only PBITEG gave intense orange-red emission; PS incorporated with OPV exhibited blue-emission, whereas a series of polymers incorporating both cross-linkers exhibited varying shades of white-light emission. One of the PS samples, PS-PBITEG-6.25-OPV-4.28 (PBITEG incorporation:  $6.25 \times 10^{-7}$  mole; OPV incorporation:  $4.28 \times 10^{-7}$  mol), exhibited pure white-light emission in the powder form with CIE coordinates (0.33, 0.32). The rigid aromatic cross-linkers were incorporated into the PS backbone in a two-stage dispersion polymerization to afford PS beads in the size range 2 to 3  $\mu\text{m}$ . The incorporation of fluorophores as cross-linkers enabled covalent attachment of the dye to the polymer backbone, avoiding dye leakage besides avoiding aggregation-induced fluorescence quenching.



## INTRODUCTION

Fluorescent materials have attracted wide attention because of their potential application in different research areas in chemistry and biology.<sup>1–4</sup> White-light-emitting luminescent materials (organic, inorganic and polymeric) have been the subject of intense research for the past decade due to their application in LEDs,<sup>5,6</sup> panel displays,<sup>7,8</sup> color-tuning materials,<sup>9,10</sup> and solid-state lighting.<sup>7,11,12</sup> The basic requirement for white-light emission is the combination of emission of the three primary colors, that is, blue, green, and red in a particular intensity that covers the visible wavelength range from 400 to 700 nm. According to the Commission Internationale d'Eclairage (CIE) chromaticity diagram,<sup>13</sup> white light can be achieved by careful tuning of contribution of each color and by varying the distance between the different dye components, leading to Förster resonance energy transfer (FRET) in the required systems.<sup>5,14–17</sup> Many researchers have developed fully organic/polymeric materials emitting white light mostly in the solution state.<sup>18–20</sup> A few reports are available for solid-state-based white-light-emitting thin films and powder based on small molecules,<sup>21,22</sup> quantum dots,<sup>23,24</sup> organogels,<sup>25,26</sup> metal organic frameworks,<sup>27</sup> nanofibers,<sup>28</sup> micro<sup>29</sup> and nanoparticles,<sup>30</sup> lanthanides,<sup>31,32</sup> and crystals.<sup>9,33</sup> Conjugated polymers based on poly(*p*-phenylenevinylene)s (PPV) and oligo(*p*-phenylenevinylene) (OPV), perylene bisimide (PBI), polythiophenes (PTh), polyfluorenes (PF), and benzthiadiazoles also have contributed toward light-harvesting systems because of their potential ability as donor and acceptor materials.<sup>10,29,34,35</sup> Supramolecular self-assembly of the donor and acceptor to achieve FRET-based white-light emission is a widely studied area

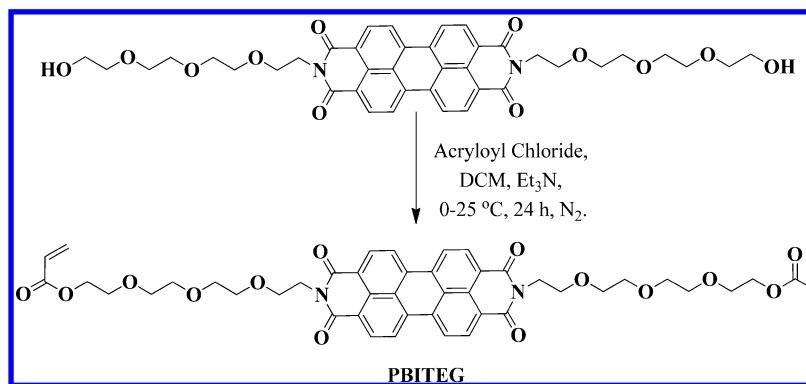
in the field of material chemistry.<sup>5,36,37</sup> Achieving white-light emission from a single polymer is quite a challenging task.<sup>38</sup> Utilizing a combination of blue-emitting oligo(fluorene), green-emitting oligo(*p*-phenylenevinylene) and red-emitting perylene, Schenning and coworkers presented the white-light-emitting hydrogen-bonded supramolecular copolymers.<sup>36,39</sup> Reports show that tunable luminescence can be obtained from silicon-linked polystyrene (PS) hybrid materials by quantum confinement effects.<sup>40–42</sup> Fluorescence quenching due to aggregation of chromophores is one of the biggest challenges plaguing the device application of most of the organic light emitting materials. Several strategies have been reported to overcome this problem in literature.<sup>43,44</sup> Controlling emission by encapsulating the dye/quantum dots in block copolymers, thereby inhibiting energy transfer, also has been a strategy for obtaining emission from pure nonaggregated species.<sup>45,46</sup> In a previous report from our group, we had shown the solid-state emission from PS beads incorporated with PBI- and OPV-based cross-linkers in a two-stage dispersion polymerization strategy.<sup>47</sup> The chromophores were isolated in the polymer matrix, thereby inhibiting aggregation-induced fluorescence quenching or FRET-based emission color tuning. Here we report tunable emission colors as well as solid-state white-light emission with high quantum yield from PS beads containing both blue-emitting OPV and orange-emitting PBI, which were covalently incorporated as cross-linkers. Single polymer-based solid-state white light (CIE

Received: May 13, 2014

Revised: July 10, 2014

Published: July 14, 2014

Scheme 1. Synthesis of Perylene-Bisimide-Based Cross-Linker (PBITEG)



coordinates;  $X = 0.33$ ,  $Y = 0.32$ ) as well as multicolor emission is reported. The isolated blue-emitting OPV and new orange-red-emitting PBI were covalently incorporated into PS beads as cross-linkers. By changing the feed ratio of both the OPV and PBITEG chromophores, we could tune the color in the solid state from blue to white and orange-red. To the best of our knowledge, this is the first example of solid-state white-light emission from a single polymer system, where chromophore isolation was used as the strategy to obtain multiple emission from different RGB components.

## MATERIALS

Perylene-3,4,9,10-tetracarboxylic dianhydride (PTCDA), zinc acetate, imidazole, poly(vinylpyrrolidone) (PVP,  $M_w$  360 000 g/mol), acrylic acid, 4-methoxyphenol, 2-ethylhexyl bromide, triethylphosphite, 4-hydroxybenzaldehyde, and potassium *tert*-butoxide were purchased from Aldrich and used without further purifications. Styrene (Aldrich) was washed with sodium hydroxide, followed by water, dried overnight using calcium chloride, and vacuum distilled before use. HBr in glacial acetic acid, *para*-formaldehyde, potassium carbonate, potassium iodide, dimethyl sulfoxide, *N,N*-dimethylformamide (DMF), tetrahydrofuran (THF), dichloromethane (DCM), and 2-chloroethanol were purchased from Merck and purified using standard procedures. Triton X-100 (70% solution in water) and 2,2'-azobis(isobutyronitrile) (AIBN) were purchased from Merck, and the latter was recrystallized from methanol.

**Measurements.**  $^{13}\text{C}$  and  $^1\text{H}$  NMR spectra were recorded in  $\text{CDCl}_3$  using Bruker AVENS 400 MHz spectrophotometer. Chemical shifts ( $\delta$ ) are reported at 298 K, with trace amount of tetramethylsilane (TMS) as internal standard. PBITEG was characterized using MALDI-TOF analysis on a Voyager-De-STRMALDI-TOF (Applied Biosystems, Framingham, MA) instrument equipped with 337 nm pulsed nitrogen laser in reflectant mode with an accelerating voltage of 25 kV. The sample in THF (micromoles) was mixed with dithranol and spotted on stainless-steel MALDI plate. The molecular-weight estimation of the polymers was carried out on a polymer lab PL-220 GPC instrument in chloroform using standards for calibration. 2 to 3 mg of the sample dissolved in chloroform was filtered and injected for recording the chromatograms at 30 °C, where the flow rate of chloroform was maintained as 1 mL. Thermal characterizations like thermogravimetric analysis (TGA) were performed using a PerkinElmer STA 6000 thermogravimetric analyzer by heating the samples from 40–800 °C at a heating rate of 10 °C/min under nitrogen. Absorption spectra were recorded using PerkinElmer Lambda 35 UV-spectrophotometer.

Steady-state fluorescence studies were performed using Horiba Jobin Yvon Fluorolog 3 spectrophotometer having a 450 W xenon lamp. The settings were as previously described.<sup>47</sup> The solid-state quantum yield was measured using a model F-3029, Quanta-Phi 6" integrating sphere connected to a Horiba Jobin Yvon Fluorolog 3 spectrophotometer. FEI, QUANTA 200 3D scanning electron microscope with tungsten filament as electron source was used for recording SEM images. Ethanol dispersion of polymer samples (1 mg/2 mL) was drop cast on silicon wafers, which were dried at room temperature in air for 12 h prior to applying a 5 nm thick gold coating. A Zetasizer ZS 90 apparatus utilizing 633 nm red laser (at 90° angle) from Malvern instruments was used for DLS measurements. A minimum of three readings were collected using freshly prepared polymer dispersions in ethanol to check for reproducibility of the data. The fluorescence microscopic images were taken by Carl Zeiss inverted fluorescence microscope model AXIO OBSERVER.ZI using DAPI (350–430 nm blue), Alexa (488–520 green), and rhodamine (480–580 nm red) filters. Polymer solutions were prepared as very dilute dispersion in ethanol, which were drop cast on glass plate, covered with coverslip and directly observed under fluorescence microscope.

**Synthesis of Perylene-Bisimide-Based Cross-Linker (PBITEG).** PBITEG was synthesized starting from PBI-TEG diol, which was synthesized as per literature procedure.<sup>48</sup> 650 mg ( $8.7 \times 10^{-4}$  mol) of PBI-TEG diol and 0.58 mL ( $4.3 \times 10^{-3}$  mol) of  $\text{Et}_3\text{N}$  were dissolved in 100 mL of dry DCM in a 250 mL of two-necked round-bottomed flask. A slow addition of acryloyl chloride (0.35 mL,  $4.3 \times 10^{-3}$  mol) in DCM was performed over a period of 15–20 min in the round-bottomed flask at 0 °C. The reaction was slowly brought to room temperature (25 °C) and allowed to stir for 24 h. The progress of the reaction was monitored using TLC. The workup of the reaction mixture was carried out by washing the organic phase with water and brine, followed by evaporation of the solvent. The compound was purified by column chromatography in DCM/methanol (1%) as solvent. Yield = 250 mg (38%).  $^1\text{H}$  NMR (200 MHz,  $\text{CDCl}_3$ ,  $\delta$ ): 8.64 (m, 8H, perylene ring), 6.35 (dd, 2H, acrylic double bond), 6.13 (q, 2H, acrylic double bond), 5.82 (dd, 2H, acrylic double bond), 4.46 (t, 4H,  $-\text{OCH}_2$ ), 4.24 (t, 4H,  $-\text{NCH}_2$ ), 3.86 (t, 4H), 3.60–3.71 (m, 20H).  $^{13}\text{C}$  NMR (500 MHz,  $\text{CDCl}_3$ ,  $\delta$ ): 165.88, 162.95, 134.01, 130.93, 13.75, 128.85, 127.97, 125.78, 122.81, 122.68, 70.41, 70.30, 69.83, 68.80, 63.39, 39.03. MALDI-TOF MS (dithranol matrix):  $m/z$  calcd for  $\text{C}_{46}\text{H}_{46}\text{N}_2\text{O}_{14}$ : 850.29; found 850.29 + 23 [ $\text{M}+\text{Na}^+$ ] 850.29 [ $\text{M}+\text{K}^+$ ].

**Table 1.** Sample Designation, Number- and Weight-Average Molar Mass, Polydispersity Indices (PDI), Yield, and 5 wt % Loss Temperature of the PS-PBITEG-X-OPV-X-Based Polymers

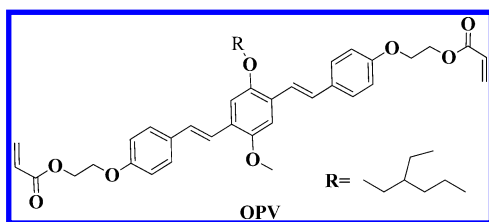
sample name	moles in feed ( $10^{-6}$ )	moles incorporated ( $10^{-7}$ ) <sup>a</sup>	yield (%)	$M_n^b$	$M_w^b$	PDI <sup>b</sup>	TGA ( $T_d = 5\%$ ) <sup>c</sup>
PS-PBITEG-6.25	3.7	6.25	93	45 900	96 800	2.1	345
PS-PBITEG-6.25-OPV-4.28	3.7	6.25	81	34 600	123 200	3.5	345
	3.7	4.28					
PS-PBITEG-4.98-OPV-3.6	3.7	4.98	90	28 500	101 700	3.5	345
	4.3	3.6					
PS-PBITEG-5.4-OPV-3.13	3.7	5.45	92	23 000	64 400	2.8	345
	3.14	3.13					
PS-PBITEG-7.4-OPV-3.71	4.3	7.4	81	27 300	115 900	4.2	345
	3.7	3.71					
PS-PBITEG-4.93-OPV-4.15	3.3	4.93	92	20 200	64 700	3.2	345
	3.7	4.15					
PS-PBITEG-3.84-OPV-4.15	2.8	3.84	86	27 900	94 800	3.4	345
	3.7	4.15					
PS-OPV-3.88	3.7	3.88	80	24 900	99 000	4	340
PS			90	40 200	124 800	3.1	320

<sup>a</sup>Measured in chloroform. <sup>b</sup>Measured by size exclusion chromatography (SEC) in chloroform ( $\text{CHCl}_3$ ), calibrated with linear, narrow molecular weight distribution poly styrene standards. <sup>c</sup>TGA measurements at heating rate of  $10^\circ\text{C}/\text{min}$  under nitrogen.

## RESULT AND DISCUSSION

**Synthesis and Characterization.** The structure of the cross-linkers used in the study and the synthesis of the fluorescent cross-linker based on perylene bisimide (PBITEG) is shown in Scheme 1. The details of the synthesis to obtain the final acryloyl functionalized PBITEG cross-linker are given in the Materials section. The synthesis of oligo(*p*-phenylenevinylene) (OPV) was previously reported by us (structure in Scheme 2).<sup>47</sup>

**Scheme 2.** Structure of Oligo(*p*-phenylenevinylene)-Based Cross-Linker (OPV)



The details of the complete structural characterization of the PBITEG cross-linker are provided in S1a–c in the Supporting Information. The two-stage dispersion polymerization procedure that we followed was described in detail in our previous publication (also provided in Supporting Information and Table S1). In short, the styrene was divided into two equal halves, and the fluorescent cross-linker was added after 1 h of polymerization along with the second half of styrene. The amounts of cross-linker were varied from 4.9 to 6.25  $\mu\text{M}$  for PBITEG and 3.13 to 4.2  $\mu\text{M}$  for OPV (0.13 to 0.51 wt % w.r.t. styrene) in the feed during the second stage of the polymerization. Two PS samples with single chromophore incorporation (either OPV or PBITEG) were also developed. The cross-linked PS with PBITEG and OPV was named as the PS-PBITEG-X-OPV-X, where 'X' indicated the amount (in micromoles) of the respective cross-linker incorporated. The incorporation of the fluorophores were too low to be detected using NMR spectroscopic techniques; therefore, absorption spectroscopy was used to estimate their incorporation based on the molar extinction coefficient of the respective cross-linker (PBITEG =  $80\,600\text{ LM}^{-1}\text{ cm}^{-1}$ , OPV =  $36\,315\text{ LM}^{-1}\text{ cm}^{-1}$ ).<sup>47</sup> The extremely

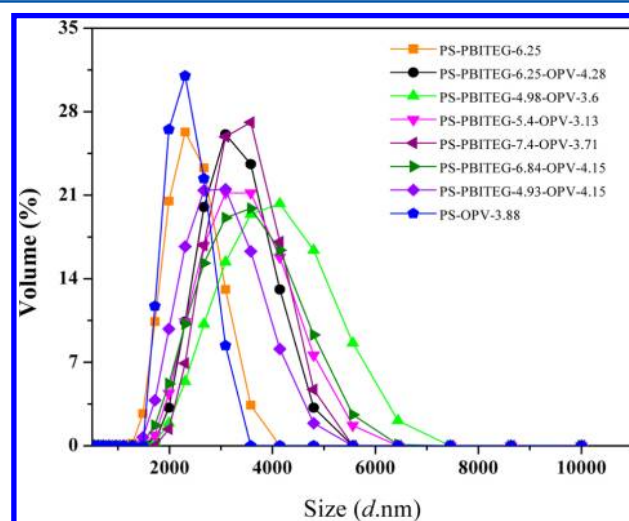


**Figure 1.** Volume-average size distribution of PS-PBITEG-X-OPV-X series in ethanol dispersion obtained by dynamic light scattering (DLS) analysis.

low incorporation ( $\sim 10^{-7}$  moles) of the cross-linkers enabled complete solubilization of the resulting lightly cross-linked polymers.<sup>49</sup> Table 1 compares the moles of fluorophore taken in feed with their actual incorporation. The molecular weight of the polymers was determined by SEC using chloroform as the eluent, and the values are given in Table 1. For comparison, the molecular weight details of PS alone prepared under identical conditions are also included in Table 1. The GPC chromatogram is given in Figure S2 in the Supporting Information. It could be seen from the Table that higher incorporation of the rigid cross-linker resulted in reduction in the  $M_w$  values. The thermal stability of the cross-linked polymers was determined by TGA carried out under a nitrogen atmosphere. Supporting Figure S3 in the Supporting Information gives the TGA plot, and Table 1 lists the 5 wt % loss temperature that was observed at 324–345  $^\circ\text{C}$ .

**Microscopic Characterization.** Dynamic light scattering (DLS) was used to estimate the particle size dispersity of the cross-linked PS beads, which were examined as ethanol dispersions. The single chromophore incorporated PS-OPV-3.88

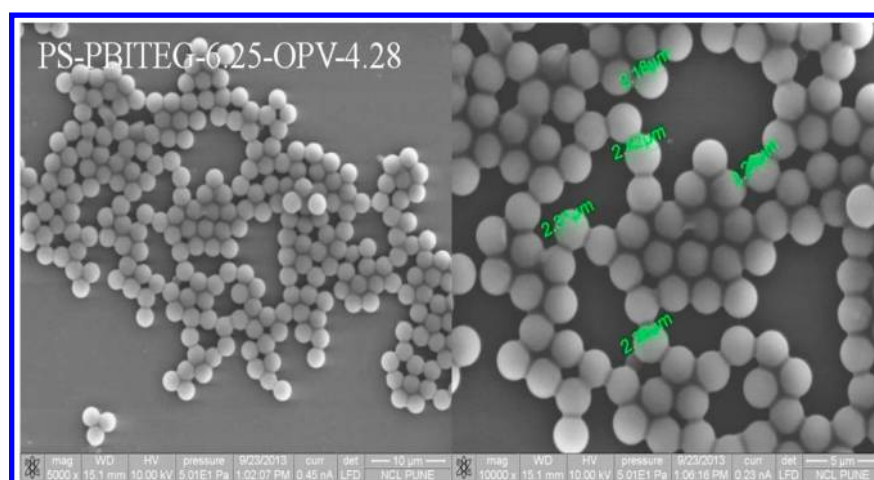


**Figure 2.** SEM image of PS-PBITEG-6.25-OPV-4.28 drop cast on silicon wafer (1 mg/2 mL ethanol dispersion) drop cast on carbon-coated copper grids.

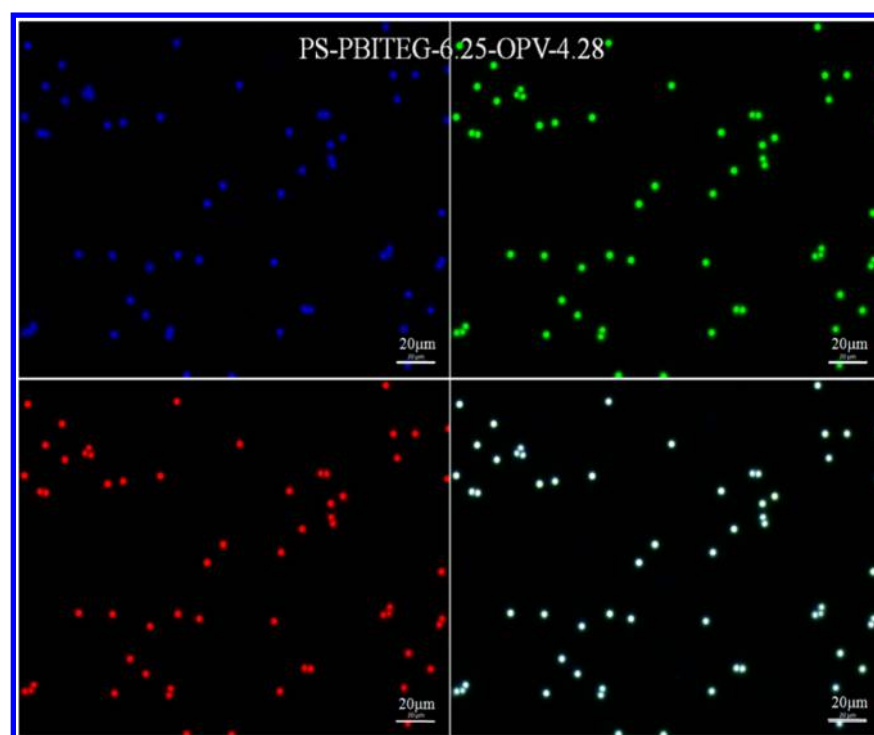


**Figure 3.** Fluorescence optical microscopy images of PS-PBITEG-6.25-OPV-4.28 using (a) DAPI (350–430 nm blue), (b) Alexa (488–520 green), and (c) rhodamine (480–580 nm red) filters and (d) merged image (white).

and PS-PBITEG-6.25 samples showed similar average particle size of 2.3  $\mu\text{m}$ , while the PS beads with both chromophores exhibited slightly higher size distribution of 3.0 to 4.0  $\mu\text{m}$ . Figure 1 shows the DLS plots for all the polymers. Figure 2 shows the SEM images of ethanol dispersed samples of PS-PBITEG-6.25-OPV-4.28 on glass substrate. It was clear that the particle size distribution observed in the SEM images was approximately similar to that obtained from DLS. Figure 3 shows the fluorescence microscope images of ethanol-dispersed samples of PS-PBITEG-6.25-OPV-4.28 on glass substrate using DAPI (350–430 nm blue), Alexa (488–520 green) and rhodamine (500–550 nm red) filters. The merged image shows white-light emission from the PS beads. The fluorescence microscope images also confirmed the size of the PS beads to be  $\sim 2.6 \mu\text{m}$ , consistent with the DLS and SEM observation. Supporting

Information (Figures S4 to S5a,b) shows the SEM and fluorescence microscope images for all PS beads with varying amounts of fluorescent cross-linker incorporation.

**Photophysical Characterization.** The absorption and emission spectra were recorded in the solid state in powder form for the polymers. Figure 4 shows images taken of the polymers under a hand-held UV lamp. PS-OPV-3.88 exhibited blue-light emission; PS-PBITEG-6.25 had yellowish orange emission, whereas the other polymers incorporating varying amounts of both fluorophore exhibited white-light emission with varying shades of whiteness intensity. The absorption spectrum of all polymers in the powder form recorded in the reflectant mode is given in the Supporting Figure S6 in the Supporting Information. Figure 5a shows the solid-state (powder form) emission spectra of the polymer PS-PBITEG-6.25-OPV-4.28 upon excitation at

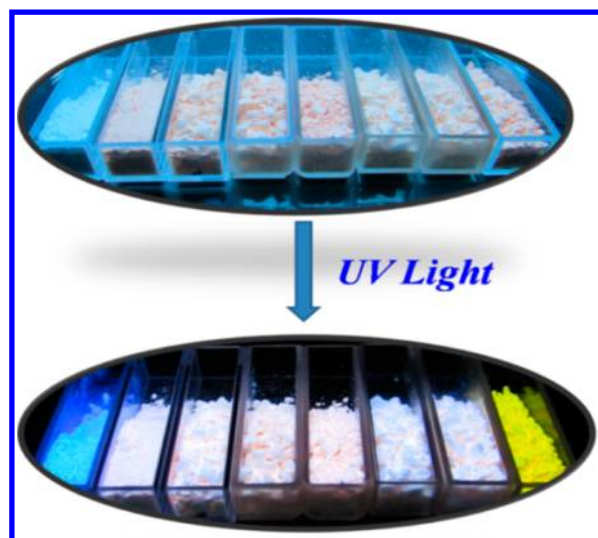


**Figure 4.** Images of the powdered samples of all polymers PS-PBITEG-X-OPV-X under (top) normal and (bottom) UV light.

350 nm. It showed peaks corresponding to OPV as well as PBITEG emission in the range 350–500 and 520–675 nm, respectively. The inset in the Figure shows the photograph of the white-light emission from the powder sample, as observed under a hand-held UV lamp. The purity of the white-light emission was assigned in photochromic terms, as standardized by Commission Internationale d'Eclairage, and the CIE coordinates were obtained as (0.33, 0.32) (Figure 5b), which was quite close to that of pure white-light emission (0.33, 0.33). The emission in the powder form of all PS samples upon excitation at 350 nm is given in Figure 6a, and their CIE chromaticity diagram is included in Figure 6b. The CIE coordinates varied from (0.15, 0.10) for the blue-emitting PS-OPV-3.88 to (0.45, 0.48) for the orange-yellow-emitting PS-PBITEG-6.25. (Values are given in Table 2.) The quantum yield for solid-state emission  $\phi_{\text{powder}}$  was measured using an integrating-sphere Quanta  $\phi$  Horiba attachment with 490 nm excitation for PBITEG and 350 nm for OPV, respectively, and the values are given in Table 2. PS-OPV-3.88 exhibited the quantum-yield value of 0.72 ( $\lambda_{\text{exc}} = 350$  nm), while PS-PBITEG-6.25 had a  $\phi_{\text{powder}}$  of 0.21 ( $\lambda_{\text{exc}} = 490$  nm). The polymers with varying incorporation of both fluorophores exhibited  $\phi_{\text{powder}}$  values ranging from 0.28 to 0.13 for blue OPV emission ( $\lambda_{\text{exc}} = 350$  nm; range 360–510 nm) and 0.26 to 0.21 for PBITEG emission in the range 500–700 nm ( $\lambda_{\text{exc}} = 490$  nm). It can be seen from Table 2 that the quantum yield for PBITEG emission was not much affected by the presence of the OPV chromophore, whereas considerable reduction was observed in the OPV emission when PBITEG was also incorporated into the PS backbone. To understand the reason for the reduction in the OPV emission quantum yield, a physical mixture of the two PS polymers having single chromophore incorporation was studied. Thus, a 1:1 (w/w) physical mixture of the two polymers PS-OPV-3.88 and PS-PBITEG-6.25 was made, and its solid-state emission spectra was compared with that of the polymer having similar molar (covalent) incorporation of both the chromophore, that is, PS-PBITEG-6.25-OPV-4.28. In Figure 7, the emission spectra of PS-OPV-3.88, PS-PBITEG-6.25-OPV-4.28, and the physical mixture of PS-OPV-3.88 and PS-PBITEG-6.25 are compared. The same spectrum after normalization at the OPV emission maxima  $\sim 430$  nm is also included in the Figure. It could be clearly observed that a

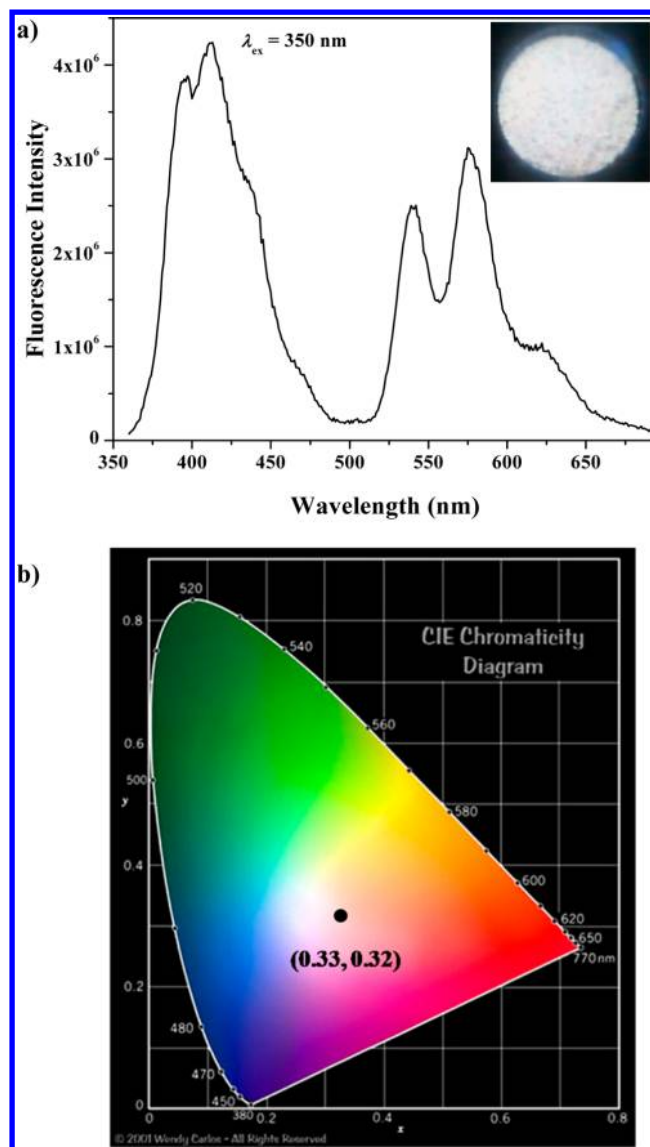


**Figure 5.** (a) Emission spectra in the solid state (powder) for PS-PBITEG-6.25-OPV-4.28 upon excitation at 350 nm. (Inset: photograph of the white emitting powder under hand-held UV lamp). (b) Corresponding CIE coordinate diagram (0.33, 0.32).

reduction in OPV emission intensity with a change in peak shape occurred in both the physical mixture (black line) and PS-PBITEG-6.25-OPV-4.28 (magenta line) compared with the OPV alone polymer PS-OPV-3.88. The Figure also shows the emission from the PBITEG alone polymer, that is, PS-PBITEG-6.25, upon excitation at 350 nm (blue line) as well as 490 nm (green line). Excitation at 350 nm corresponding to the OPV absorption maxima also resulted in excitation of PBITEG; selective excitation of OPV was not possible in the system. Figure 8 shows the excitation spectra of PS-PBITEG-6.25-OPV-4.28, PS-PBITEG-6.25, and the physical mixture of PS-OPV-3.88 and PS-PBITEG-6.25, collected at 576 nm. The Figure also shows the excitation spectra collected for PS-OPV-3.88 at 433 nm. The absence of OPV absorption from the PS-PBITEG-6.25-OPV-4.28 as well as the physical mixture of PS-OPV-3.88 and PS-PBITEG-6.25 demonstrated the absence of energy transfer between the OPV and PBITEG chromophores. The comparison of excitation spectrum of all polymers with PS-OPV-3.88 and PS-PBITEG-6.25-PS-OPVA-4.28 is also

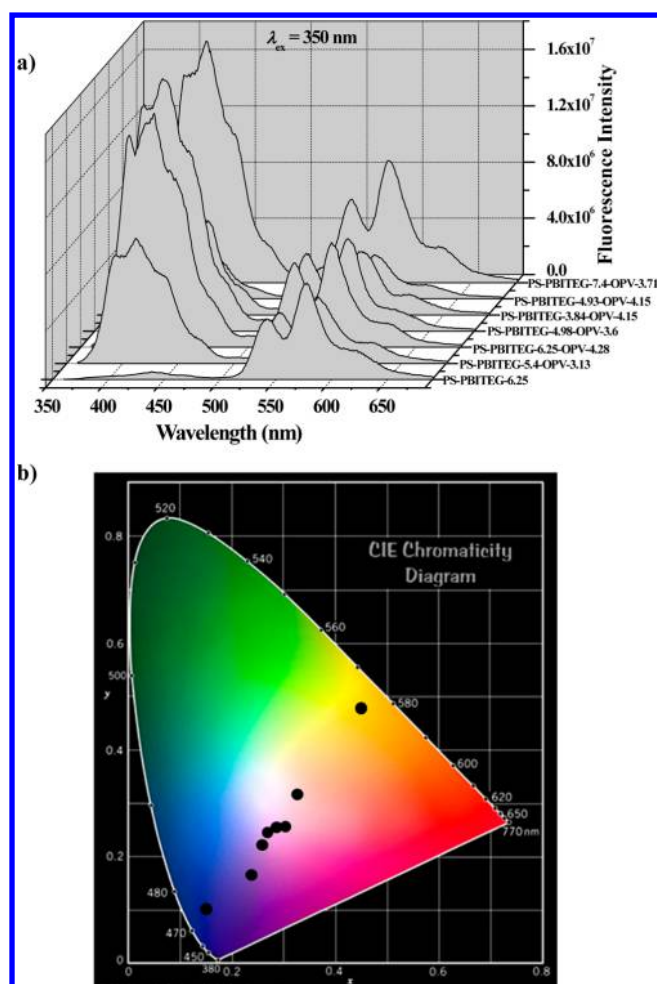


**Figure 6.** (a) Solid-state (powder) emission spectra of the cross-linked PS-PBITEG-X-OPV-X series upon excitation at 350 nm and (b) corresponding CIE coordinate diagram.

**Table 2. Photoluminescence Quantum Yield in Powder Form and Corresponding CIE Coordinates**

sample name	solid-state quantum yield ( $\phi$ )		CIE color coordinate	
	$\lambda_{\text{ex}}=350\text{nm}$	$\lambda_{\text{ex}}=490\text{nm}$	X	Y
OPV-cross-linker	0.02			
PBITEG-cross-linker		0.06		
PS-OPV-3.88	0.72		0.15	0.1
PS-PBITEG-6.25		0.21	0.45	0.48
PS-PBITEG-5.4-OPV-3.13	0.22 <sup>a</sup>	0.23 <sup>b</sup>	0.30	0.26
PS-PBITEG-6.25-OPV-4.28	0.13 <sup>a</sup>	0.23 <sup>b</sup>	0.33	0.32
PS-PBITEG-4.98-OPV-3.6	0.27 <sup>a</sup>	0.25 <sup>b</sup>	0.29	0.24
PS-PBITEG-3.84-OPV-4.15	0.28 <sup>a</sup>	0.26 <sup>b</sup>	0.26	0.22
PS-PBITEG-4.93-OPV-4.15	0.26 <sup>a</sup>	0.25 <sup>b</sup>	0.28	0.24
PS-PBITEG-7.4-OPV-3.71	0.18 <sup>a</sup>	0.21 <sup>b</sup>	0.30	0.26
PS-PBITEG-6.25+PS-OPV-3.88 (Physical Mix)			0.24	0.18

<sup>a</sup>Selected wavelength range: 360–510 nm. <sup>b</sup>Selected wavelength range: 500–700 nm.

given in the Figure S7 in the Supporting Information. These facts suggested that energy transfer from OPV to PBITEG could not have been the reason for the observed change of shape of the OPV emission spectra as well as the observation of PBITEG emission upon excitation of the OPV chromophore. Fluorescence

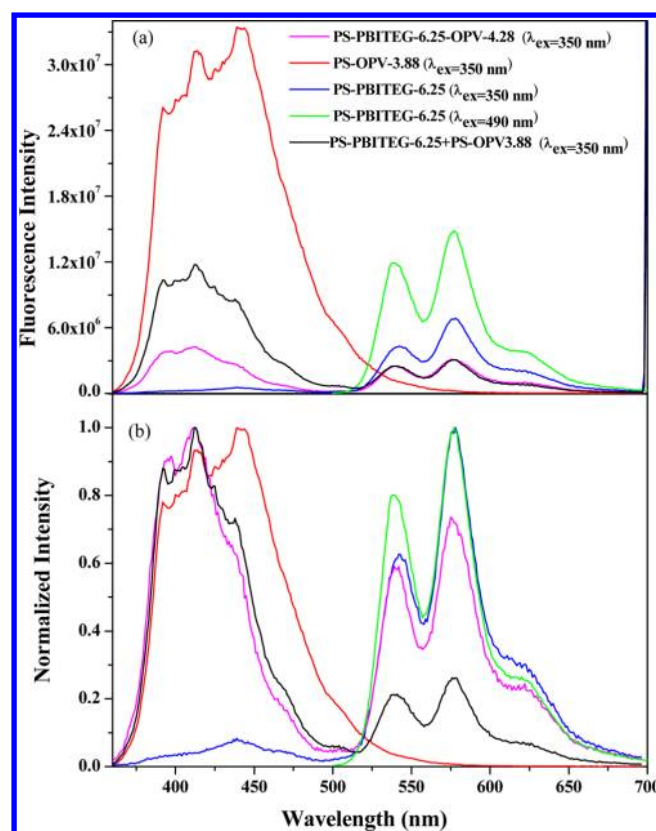


**Figure 7.** (a) Solid-state emission spectra upon excitation at 350 nm for PS-OPV-3.88, PS-PBITEG-6.25-OPV-4.28, physical mixture of PS-PBITEG-6.25+PS-OPV-3.88, along with that of PS-PBITEG-3.2 (excitation at 490 nm). (b) Same spectra after normalization at the OPV emission maxima of  $\sim 430$  nm.

emission lifetime decay studies were undertaken by excitation using a LED of 339 nm, and collecting the data at 412 nm. Supporting Figure S8 in the Supporting Information shows the lifetime decay profiles of four polymers PS-OPV-3.88, PS-PBITEG-3.84-OPV-4.15, PS-PBITEG-4.93-OPV-4.15, and PS-PBITEG-7.4-OPV-3.71 in the powder state, and the fit values are given in Supporting Table S2 in the Supporting Information. Although the decay of all polymers were best fitted using a triexponential fit, the most prominent species ( $\alpha_3 = 0.98$ ) in the OPV alone polymer, PS-OPV-3.88, had a lifetime of 0.1 ns. The lifetime decay of the polymers with both OPV and PBITEG incorporation was complicated by more than two species that decayed with different lifetimes. The fact that selective excitation of OPV chromophore alone was not possible using excitation source near 340 nm could be the reason for the presence of multiple emitting species. Thus, the fluorescence lifetime decay data could not give a conclusive evidence of absence of energy transfer. However, one more indirect evidence of absence of energy transfer to be the cause of the reduction in fluorescence emission intensity and change in shape of emission from OPV was obtained by comparing the emission spectra of the OPV alone polymer in the form of thin drop cast film as well as in powder. Figure 9 compares the normalized (at 412 nm) emission spectra of the OPV alone polymer PS-OPV-3.88 collected both in the powder form as well as drop cast from chloroform. A change in peak shape as well as reduction in fluorescence intensity was observed for the chloroform drop cast film similar to that observed for the PS-PBITEG-OPV polymers.

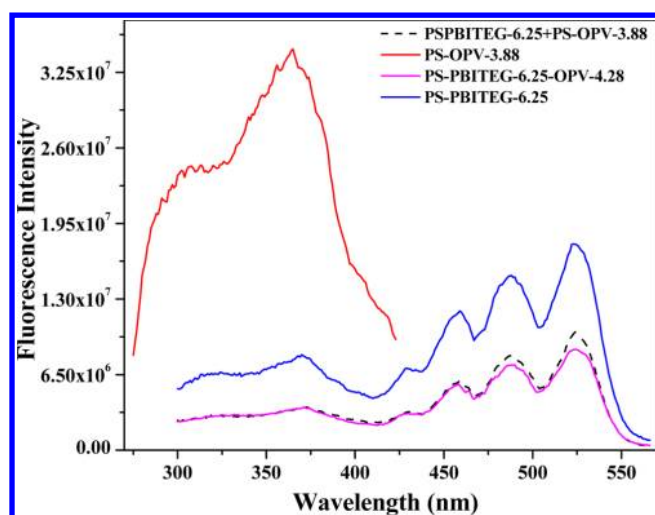


**Figure 8.** Solid-state excitation spectra collected at 433 nm for PS-OPV-3.88 and at 576 nm for PS-PBITEG-6.25-OPV-4.28 and PS-PBITEG-6.25. The excitation spectrum of the physical mixture of PS-PBITEG-6.25+PS-OPV-3.88 is also given for comparison.

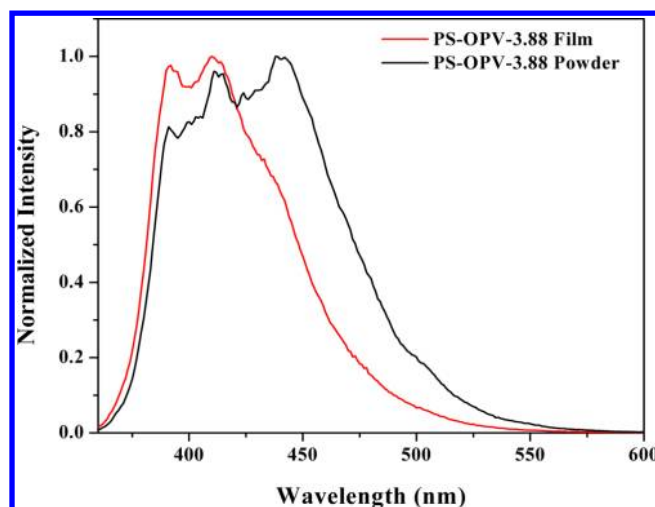


**Figure 9.** Comparison of solid state emission spectra of PS-OPV-3.8 in the powder form and as drop cast film from  $\text{CHCl}_3$  upon excitation at 350 nm.

These data indicated that the OPV chromophore was extremely sensitive to the surrounding, and some changes in the packing might be the cause of this change in the shape of the emission spectra collected in the film compared with that in powder.<sup>50</sup> The influence of the aromatic styrene rings of the PS backbone affecting the packing of the OPV rings also cannot be ruled out. We had previously demonstrated that incorporation of the OPV cross-linker into a nonaromatic polymer backbone like that of poly(methyl methacrylate) (PMMA) did not exhibit any shift or change of shape of the OPV chromophore absorption or emission in solution.<sup>47</sup> However, when PBITEG was also introduced into the backbone of PMMA along with OPV (details of synthesis are given in the Supporting Information), drastic changes in the emission of the OPV chromophore was observed in powder form. Figure 10 compares the emission spectra recorded in the powder form for PMMA-OPV-2.5 and PMMA-PBITEG-2.6-OPV-2.5 polymers upon excitation at 350 nm. The spectrum of PS-OPV-3.88 is also given for comparison. Nearly  $\sim 18$  nm blue shift was observed for the OPV emission in

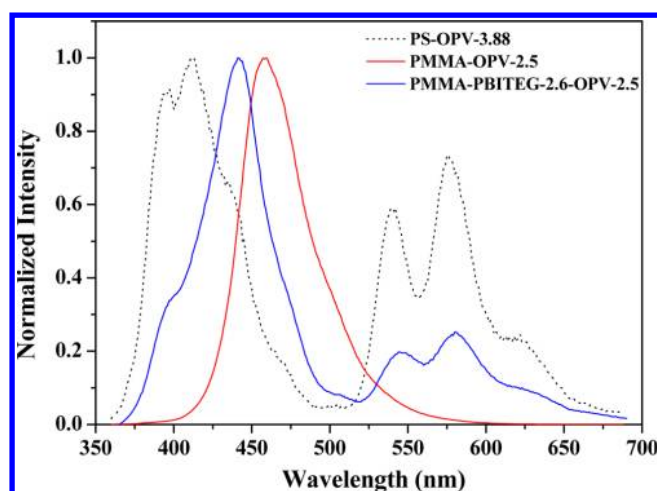


**Figure 10.** Comparison of solid-state (powder) emission spectra of PS-OPV-3.88 with that of PMMA-OPV-2.5 and PMMA-PBITEG-2.6-OPV-2.5 upon excitation at 350 nm.

the presence of PBITEG (459 nm for PMMA-OPV-2.5 vs 441 nm for PMMA-PBITEG-2.6-OPV-2.5), although no shift was observed for the PBI emission. It was thus evident that OPV as a chromophore was extremely sensitive to its environment as well as packing, whether it was stacked tightly along with similar aromatic core like PS or packing influenced by the nature of the solvent from which it was drop cast to form film or by the presence of other chromophores like PBI in the vicinity. This change in the environment or packing was reflected as a change in the extent of aggregation, leading to fluorescence quenching and change in spectral pattern in the powder form in the PS-PBITEG-X-OPV-X polymers.

## CONCLUSIONS

In summary, we have demonstrated single-polymer-based white-light and multicolor emission in the solid state. Fluorescent microbeads in the size range of 2 to 3  $\mu\text{m}$  were produced by incorporating orange-red emitting PBI and blue emitting oligo(*p*-phenylenevinylene) as cross-linkers into the polymer backbone. Pure white-light emission in the powder form with CIE coordinates (0.33, 0.32) was achieved with one of the PS samples having appropriate amounts of OPV and PBITEG - (PS-PBITEG-6.25-OPV-4.28). The two-stage dispersion polymerization method along with the concept of fluorophore as covalent cross-linker for chromophore isolation affords an easy and scalable method to produce fluorescently labeled polymer particles with controlled size from commercial polymers like PS.

## ASSOCIATED CONTENT

### Supporting Information

Details of structural characterization of the monomers and polymers. This material is available free of charge via the Internet at <http://pubs.acs.org>.

## AUTHOR INFORMATION

### Notes

The authors declare no competing financial interest.

## ACKNOWLEDGMENTS

We thank Dr B.L.V. Prasad, Mr. Ketan Bhotkar, and Dr Neetu Singh, NCL – Pune, for reflectant mode absorption spectra, SEM, and fluorescence microscope facility, respectively. We thank IISER-Pune

for the DLS measurements. S.L.S. thanks CSIR-New Delhi, India for Senior Research Fellowship.

## REFERENCES

- (1) Schubert, E. F.; Kim, J. K. Solid-State Light Sources Getting Smart. *Science* **2005**, *308*, 1274–1278.
- (2) Han, M.; Gao, X.; Su, J. Z.; Nie, S. Quantum-Dot-Tagged Microbeads for Multiplexed Optical Coding of Biomolecules. *Nat. Biotechnol.* **2001**, *19*, 631–635.
- (3) Hudson, Z. M.; Lunn, D. J.; Winnik, M. A.; Manners, I. Colour-Tunable Fluorescent Multiblock Micelles. *Nat. Commun.* **2014**, 1–8.
- (4) Sukhanova, A.; Nabiev, I. Fluorescent Nanocrystal-Encoded Microbeads for Multiplexed Cancer Imaging and Diagnosis. *Crit. Rev. Oncol./Hematol.* **2008**, *68*, 39–59.
- (5) Huang, C.-H.; Chiu, Y.-C.; Yeh, Y. T.; Chan, T.-S.; Chen, T.-M. Eu<sup>2+</sup>-Activated Sr<sub>8</sub>ZnSc(PO<sub>4</sub>)<sub>7</sub>: A Novel Near-Ultraviolet Converting Yellow-Emitting Phosphor for White Light-Emitting Diodes. *ACS Appl. Mater. Interfaces* **2012**, *4*, 6661–6668.
- (6) Babu, S. S.; Praveen, V. K.; Ajayaghosh, A. Functional  $\pi$ -Gels and their Applications. *Chem. Rev.* **2014**, *114*, 1973–2129.
- (7) Wu, H.; Ying, L.; Wei, Y.; Cao, Y. Progress and Perspective of Polymer White Light-Emitting Devices and Materials. *Chem. Soc. Rev.* **2009**, *38*, 3391–3400.
- (8) D'Andrade, B. W.; Forrest, S. R. White Organic Light Emitting Devices for Solid-State Lighting. *Adv. Mater.* **2004**, *16*, 1585–1595.
- (9) Fang, X.; Roushan, M.; Zhang, R.; Peng, J.; Zeng, H.; Li, J. Tuning and Enhancing White Light Emission of II–VI Based Inorganic–Organic Hybrid Semiconductors as Single-Phased Phosphors. *Chem. Mater.* **2012**, *24*, 1710–1717.
- (10) Yan, D.; Lu, J.; Ma, J.; Wei, M.; Evans, D. G.; Duan, X. Reversibly Thermochromic, Fluorescent Ultrathin Films with a Supramolecular Architecture. *Angew. Chem., Int. Ed.* **2011**, *50*, 720–723.
- (11) Farinola, G. M.; Ragni, R. Electroluminescent Materials for White Organic Light Emitting Diodes. *Chem. Soc. Rev.* **2011**, *40*, 3467–3482.
- (12) Kamtekar, K. T.; Monkman, A. P.; Bryce, M. R. Recent Advances in White Organic Light-Emitting Materials and Devices (WOLEDs). *Adv. Mater.* **2010**, *22*, 572–582.
- (13) <http://hyperphysics.phy-astr.gsu.edu/hbase/vision/cie.html#c2> (accessed on June 12, 2010).
- (14) Chen, Z.; Grumstrup, E. M.; Gilligan, A. T.; Papanikolas, J. M.; Schanze, K. S. Light-Harvesting Polymers: Ultrafast Energy Transfer in Polystyrene-Based Arrays of  $\pi$ -Conjugated Chromophores. *J. Phys. Chem. B* **2014**, *118*, 372–378.
- (15) Ajayaghosh, A.; Praveen, V. K.; Vijayakumar, C. Organogels as Scaffolds for Excitation Energy Transfer and Light Harvesting. *Chem. Soc. Rev.* **2008**, *37*, 109–122.
- (16) Maiti, D. K.; Bhattacharjee, R.; Datta, A.; Banerjee, A. Modulation of Fluorescence Resonance Energy Transfer Efficiency for White Light Emission from a Series of Stilbene-Perylene Based Donor–Acceptor Pair. *J. Phys. Chem. C* **2013**, *117*, 23178–23189.
- (17) Wang, T.; Chirmanov, V.; Chiu, W. H. M.; Radovanovic, P. V. Generating Tunable White Light by Resonance Energy Transfer in Transparent Dye-Conjugated Metal Oxide Nanocrystals. *J. Am. Chem. Soc.* **2013**, *135*, 14520–14523.
- (18) Zhang, X.; Görl, D.; Würthner, F. White-Light Emitting Dye Micelles in Aqueous Solution. *Chem. Commun.* **2013**, *49*, 8178–8180.
- (19) Vijayakumar, C.; Sugiyasu, K.; Takeuchi, M. Oligofluorene-based Electrophoretic Nanoparticles in Aqueous Medium as a Donor Scaffold for Fluorescence Resonance Energy Transfer and White-Light Emission. *Chem. Sci.* **2011**, *2*, 291–294.
- (20) Roushan, M.; Zhang, X.; Li, J. Solution-Processable White-Light-Emitting Hybrid Semiconductor Bulk Materials with High Photoluminescence Quantum Efficiency. *Angew. Chem., Int. Ed.* **2012**, *51*, 436–439.
- (21) Chang, Y.-T.; Chang, J.-K.; Lee, Yi.-T.; Wang, Po.-S.; Wu, J.-L.; Hsu, Che.-C.; Wu, I.-W.; Tseng, Wei.-H.; Pi, T.-W.; Chen, C.-T.; et al. High-Efficiency Small-Molecule-Based Organic Light Emitting Devices with Solution Processes and Oxadiazole-Based Electron Transport Materials. *ACS Appl. Mater. Interfaces* **2013**, *5*, 10614–10622.
- (22) Wang, X.; Chang, Yi.-Lu.; Lu, J.-S.; Zhang, T.; Lu, Z.-H.; Wang, S. Bright Blue and White Electrophosphorescent Triarylboryl-Functionalized  $\bar{C}N$ -Chelate Pt(II) Compounds: Impact of Intramolecular Hydrogen Bonds and Ancillary Ligands. *Adv. Funct. Mater.* **2014**, *24*, 1911–1927.
- (23) Liang, R.; Yan, D.; Tian, R.; Yu, X.; Shi, W.; Li, C.; Wei, M.; Evans, D. G.; Duan, X. Quantum Dots-Based Flexible Films and Their Application as the Phosphor in White Light-Emitting Diodes. *Chem. Mater.* **2014**, *26*, 2595–2600.
- (24) Sohn, I. S.; Unithrattil, S.; Im, W. B. Stacked Quantum Dot Embedded Silica Film on a Phosphor Plate for Superior Performance of White Light-Emitting Diodes. *ACS Appl. Mater. Interfaces* **2014**, *6*, 5744–5748.
- (25) Bairi, P.; Roy, B.; Chakraborty, P.; Nandi, A. K. Co-assembled White-Light-Emitting Hydrogel of Melamine. *ACS Appl. Mater. Interfaces* **2013**, *5*, 5478–5485.
- (26) Chen, Q.; Zhang, D.; Zhang, G.; Yang, X.; Feng, Y.; Fan, Q.; Zhu, D. Multicolor Tunable Emission from Organogels Containing Tetraphenylethene, Peryleneimide, and Spiropyran Derivatives. *Adv. Funct. Mater.* **2010**, *20*, 3244–3251.
- (27) Sun, C.-Y.; Wang, X.-L.; Zhang, Xi.; Qin, C.; Li, P.; Su, Z.-M.; Zhu, D.-X.; Shan, G.-G.; Shao, K.-Z.; Wu, H.; Li, J. Efficient and Tunable White-Light Emission of Metal–Organic Frameworks by Iridium-Complex Encapsulation. *Nat. Commun.* **2013**, 1–8.
- (28) Giansante, C.; Raffy, G.; Schäfer, C.; Rahma, H.; Kao, M.-T.; Olive, A. G. L.; Guerso, A. D. White-Light-Emitting Self-Assembled Nanofibers and Their Evidence by Microspectroscopy of Individual Objects. *J. Am. Chem. Soc.* **2011**, *133*, 316–325.
- (29) Narayana, Y. S. L. V.; Basak, S.; Baumgarten, M.; Müllen, K.; Chandrasekar, R. White-Emitting Conjugated Polymer/Inorganic Hybrid Spheres: Phenylethynyl and 2,6-Bis(pyrazolyl) pyridine Copolymer Coordinated to Eu(tta)<sub>3</sub>. *Adv. Funct. Mater.* **2013**, *23*, 5875–5880.
- (30) Tseng, K.-P.; Fang, F.-C.; Shyue, J.-J.; Wong, K.-T.; Raffy, G.; Guerso, A. D.; Bassani, D. M. Spontaneous Generation of Highly Emissive RGB Organic Nanospheres. *Angew. Chem., Int. Ed.* **2011**, *50*, 7032–7036.
- (31) Balamurugan, A.; Reddy, M. L. P.; Jayakannan, M. Single Polymer Photosensitizer for Tb<sup>3+</sup> and Eu<sup>3+</sup> ions: A Novel Approach for White Light Emission based on Carboxylic Functionalized Poly(m-phenylenevinylene)s. *J. Phys. Chem. B* **2009**, *113*, 14128–14138.
- (32) Huang, C.-H.; Liu, Wei.-R.; Chen, T.-M. Single-Phased White-Light Phosphors Ca<sub>9</sub>Gd(PO<sub>4</sub>)<sub>7</sub>:Eu<sup>2+</sup>,Mn<sup>2+</sup> under Near-Ultraviolet Excitation. *J. Phys. Chem. C* **2010**, *114*, 18698–18701.
- (33) Dukes, A. D.; Samson, P. C.; Keene, J. D.; Davis, L. M.; Wikswo, J. P.; Rosenthal, S. J. Single-Nanocrystal Spectroscopy of White-Light-Emitting CdSe Nanocrystals. *J. Phys. Chem. A* **2011**, *115*, 4076–4081.
- (34) Ego, C.; Marsitzky, D.; Becker, S.; Zhang, J.; Grimdale, A. C.; Mullen, K.; MacKenzie, J. D.; Silva, C.; Friend, R. H. Attaching Perylene Dyes to Polyfluorene: Three Simple, Efficient Methods for Facile Color Tuning of Light-Emitting Polymers. *J. Am. Chem. Soc.* **2003**, *125*, 437–443.
- (35) Liu, J.; Guo, X.; Bu, L.; Xie, Z.; Cheng, Y.; Geng, Y.; Wang, L.; Jing, X.; Wang, F. White Electroluminescence from a Single-Polymer System with Simultaneous Two-Color Emission: Polyfluorene as Blue Host and 2,1,3-Benzothiadiazole Derivatives as Orange Dopants on the Side Chain. *Adv. Funct. Mater.* **2007**, *17*, 1917–1925.
- (36) Abbel, R.; van der Weegen, R.; Pisula, W.; Surin, M.; Leclre, P.; Lazzaroni, R.; Meijer, E. W.; Schenning, A. P. H. J. Multicolour Self-Assembled Fluorene Co-Oligomers: From Molecules to the Solid State via White-Light-Emitting Organogels. *Chem.—Eur. J.* **2009**, *15*, 9737–9746.
- (37) Praveen, V. K.; Ranjith, C.; Bandini, E.; Ajayaghosh, A.; Armaroli, N. Oligo(phenylenevinylene) Hybrids and Self-assemblies: Versatile Materials for Excitation Energy Transfer. *Chem. Soc. Rev.* **2014**, *43*, 4222–4242.
- (38) Tu, G.; Mei, C.; Zhou, Q.; Cheng, Y.; Geng, Y.; Wang, L.; Ma, D.; Jing, X.; Wang, F. Highly Efficient Pure-White-Light-Emitting Diodes

from a Single Polymer: Polyfluorene with Naphthalimide Moieties. *Adv. Funct. Mater.* **2006**, *16*, 101–106.

(39) Abbel, R.; Grenier, C.; Pouderoijen, M. J.; Stouwdam, J. W.; Leclère, P. E. L. G.; Sijbesma, R. P.; Meijer, E. W.; Schenning, A. P. H. J. White-Light Emitting Hydrogen-Bonded Supramolecular Copolymers Based on  $\pi$ -Conjugated Oligomers. *J. Am. Chem. Soc.* **2009**, *131*, 833–843.

(40) Yang, Z.; Dasog, M.; Dobbie, A. R.; Lockwood, R.; Zhi, Y.; Meldrum, A.; Veinot, J. G. C. Highly Luminescent Covalently Linked Silicon Nanocrystal/Polystyrene Hybrid Functional Materials: Synthesis, Properties, and Processability. *Adv. Funct. Mater.* **2014**, *24*, 1345–1353.

(41) Harun, N. A.; Benning, M. J.; Horrocks, B. R.; Fulton, D. A. Gold Nanoparticle-Enhanced Luminescence of Silicon Quantum Dots Co-Encapsulated in Polymer Nanoparticles. *Nanoscale* **2013**, *5*, 3817–3827.

(42) Wu, X. L.; Fan, J. Y.; Qui, T.; Yang, X.; Siu, G. G.; K, C.; Chu, P. K. Experimental Evidence for the Quantum Confinement Effect in 3C-SiC Nanocrystallites. *Phys. Rev. Lett.* **2005**, *94*, 026102.

(43) Lee, H. M.; Kim, Y. N.; Kim, B. H.; Kim, S. O.; Cho, S. O. Fabrication of Luminescent Nanoarchitectures by Electron Irradiation of Polystyrene. *Adv. Mater.* **2008**, *20*, 2094–2098.

(44) Wang, R.; Peng, J.; Qiu, F.; Yang, Y. Enhanced White-light Emission from Multiple Fluorophores Encapsulated in a Single Layer of Diblock Copolymer Micelles. *Chem. Commun.* **2011**, *47*, 2787–2789.

(45) Yoo, S.; An, S. J.; Choi, G. H.; Kim, K. S.; Yi, G.-C.; Zin, W.-C.; Jung, J. C.; Sohn, B.-H. Controlled Light Emission by Nano-encapsulation of Fluorophores in Thin Films of Diblock Copolymer Micelles. *Adv. Mater.* **2007**, *19*, 1594–1596.

(46) Park, S.; Kwon, J. E.; Kim, S. H.; Seo, J.; Chung, K.; Park, S.-Y.; Jang, Du-J.; Medina, B. M.; Gierschner, J.; Park, S. Y. A White-Light-Emitting Molecule: Frustrated Energy Transfer between Constituent Emitting Centers. *J. Am. Chem. Soc.* **2009**, *131*, 14043–14049.

(47) Sonawane, S. L.; Asha, S. K. Fluorescent Cross-Linked Polystyrene Perylenebisimide/ Oligo (*p*-Phenylenevinylene) Microbeads with Controlled Particle Size, Tunable Colors, and High Solid State Emission. *ACS Appl. Mater. Interfaces* **2013**, *5*, 12205–12214.

(48) Wang, W.; Li, L.-S.; Helms, G.; Zhou, H.-H.; Li, A. D. Q. Reversibly Photoswitchable Dual-Color Fluorescent Nanoparticles as a New Tool for Live Cell Imaging. *J. Am. Chem. Soc.* **2003**, *125*, 1120–1121.

(49) *Water Soluble Polymers Solution Properties and Applications*; Amjad, Z., Ed.; Plenum Press: New York, 1998.

(50) Amrutha, S. R.; Jayakannan, M. Structure Control of  $\pi$ -Conjugated Polymers for Enhanced Solid-State Luminescence: Synthesis and Liquid Crystalline and Photophysical Properties of New Bulky Poly(*p*-phenylenevinylene)s and Oligo(phenylenevinylene)s Bearing Tricyclodecane Pendant. *Macromolecules* **2007**, *40*, 2380–2391.